Inorganic Chemistry

Article

pubs.acs.org/IC

Relationship between Oxygen Affinity and Autoxidation of Myoglobin

Tomokazu Shibata,[†] Daichi Matsumoto,[†] Ryu Nishimura,[†] Hulin Tai,[†] Ariki Matsuoka,[‡] Satoshi Nagao,[§] Takashi Matsuo,[§] Shun Hirota,[§] Kiyohiro Imai,[∥] Saburo Neya,[⊥] Akihiro Suzuki,[#] and Yasuhiko Yamamoto*[,†]

[†]Department of Chemistry, University of Tsukuba, Tsukuba 305-8571, Japan

[‡]Fukushima Medical University, Fukushima 960-1295, Japan

[§]Graduate School of Materials Science, Nara Institute of Science and Technology, Ikoma, Nara 630-0192, Japan

[∥]Department of Frontier Bioscience, Faculty of Bioscience and Applied Chemistry, Hosei University, Koganei, Tokyo 184-8584, Japan

[⊥]Department of Physical Chemistry, Graduate School of Pharmaceutical Sciences, Chiba University, Inage-Yayoi, Chiba 263-8522, Japan

[#]Department of Materials Engineering, Nagaoka National College of Technology, Nagaoka 940-8532, Japan

Supporting Information

ABSTRACT: Studies using myoglobins reconstituted with a variety of chemically modified heme cofactors revealed that the oxygen affinity and autoxidation reaction rate of the proteins are highly correlated to each other, both decreasing with decreasing the electron density of the heme iron atom. An $Fe^{3+}-O_2^-$-like species has been expected for the $Fe^{2+}-O_2$ bond in the protein, and the electron density of the heme iron atom influences the resonance process between the two forms. A shift of the resonance toward the $Fe^{2+}-O_2$ form results in lowering of the O_2 affinity due to an increase in the O_2 dissociation rate. On the other hand, a shift of the resonance toward the $Fe^{3+}-O_2^-$-like species results in acceleration of the autoxidation through increasing H^+ affinity of the bound ligand.

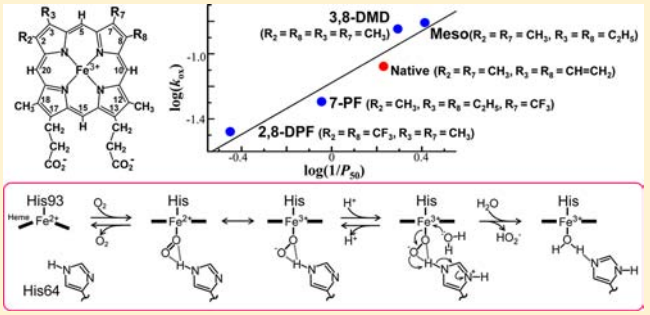

INTRODUCTION

Myoglobin (Mb), an oxygen storage hemoprotein, is at present the best, albeit incompletely, understood protein in terms of its structure and function.[1−8] O_2 binds reversibly to the ferrous heme Fe atom (Fe(II)) in Mb. During this reversible O_2 binding, the Fe(II) state has to be maintained in the protein, because the ferric heme Fe atom (Fe(III)) is incapable of binding O_2 and hence is physiologically inactive. The Fe(II) state of the oxygenated protein tends to be oxidized readily into the Fe(III) one through a process known as "autoxidation".[9] In fact, an enzymatic reduction system is present *in situ* to regenerate the Fe(II) state from the Fe(III) one.[10] Thus, understanding of the Mb function demands elucidation of the mechanisms responsible for control of both its O_2 affinity and autoxidation.

Olson and his associates[4,11−14] have investigated a great variety of artificial mutants in order to elucidate the mechanistic relationship between the O_2 affinity and autoxidation of Mb. They found that Mb possessing lower O_2 affinity exhibits a larger autoxidation reaction rate (k_{ox}), and hence inferred that it is difficult to construct O_2-binding hemoproteins with low O_2 affinity and small k_{ox} values, which are a prerequisite for engineering hemoprotein-based blood substitutes.[11]

In order to elucidate the relationship between the functional properties of Mb and its heme electronic structure, we previously studied proteins reconstituted with various heme cofactors such as mesoheme (Meso), 13,17-bis(2-carboxylatoethyl)-3,8-diethyl-2,12,18-trimethyl-7-trifluoromethylporphyrinatoiron(III)[15] (7-PF), and 13,17-bis(2-carboxylatoethyl)-3,7-diethyl-12,18-trimethyl-2,8-ditrifluoromethylporphyrinatoiron(III)[16] (2,8-DPF) (Figure 1), that is, Mb(Meso), Mb(7-PF), and Mb(2,8-DPF), respectively. The electron density of the heme Fe atom (ρ_{Fe}) in the protein has been estimated on the basis of the equilibrium constant (pK_a) of the so-called "acid−alkaline transition" in metmyoglobin (metMb) (Scheme 1).[3,17−20] In metMb possessing highly conserved distal His64, H_2O and OH^- are coordinated to the heme Fe under low and high pH conditions, respectively,[3] and hence the ρ_{Fe} value is manifested in the

Received: August 23, 2012
Published: October 19, 2012

   dx.doi.org/10.1021/ic301848t | Inorg. Chem. 2012, 51, 11955−11960

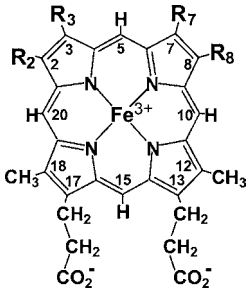

Figure 1. Structures and numbering system for the heme cofactors used in the study. Proto ($R_2 = R_7 = CH_3$, $R_3 = R_8 = CH{=}CH_2$), meso ($R_2 = R_7 = CH_3$, $R_3 = R_8 = C_2H_5$), 3,8-DMD ($R_2 = R_8 = R_3 = R_7 = CH_3$), 7-PF ($R_2 = CH_3$, $R_3 = R_8 = C_2H_5$, $R_7 = CF_3$), and 2,8-DPF ($R_2 = R_8 = CF_3$, $R_3 = R_7 = CH_3$).

Scheme 1. Acid−Alkaline Transition in metMb

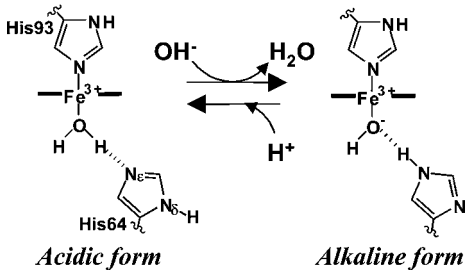

pK_a one through its effect on the H^+ affinity of the Fe^{3+}-bound OH^-. Analysis indicated that the proteins can be ranked as Mb(2,8-DPF) < Mb(7-PF) < Native Mb < Mb(Meso), in order of increasing ρ_{Fe} value. We found that the O_2 affinity of Mb is regulated by the ρ_{Fe} value in such a manner that the O_2 affinity of the protein decreases, due to an increase in the O_2 dissociation rate, with a decrease in the ρ_{Fe} value.[16]

In the present study, we determined the k_{ox} values of these four proteins as well as the protein reconstituted with 3,8-dimethyl-deuteroporphyrinatoiron(III)[21,22] (3,8-DMD) (Figure 1), that is, Mb(3,8-DMD), under acidic pH conditions. The study revealed that the k_{ox} value is also regulated by the ρ_{Fe} value in such a manner that the k_{ox} value decreases with decreasing ρ_{Fe} value. In addition, in order to characterize the O_2 affinity of Mb(3,8-DMD), the P_{50} value, which is the partial pressure of O_2 required to achieve 50% oxygenation, was also determined, and the determined value agreed well with the one predicted from the previously reported relationship between the O_2 affinity and pK_a value, and hence the ρ_{Fe} one,[16] further supporting the regulation of the O_2 affinity of the protein through the ρ_{Fe} value. Consequently, the present study demonstrated that decreases in both the O_2 affinity and the k_{ox} value of Mb can be simultaneously achieved through a decrease in the ρ_{Fe} value. Thus, this study provides a new way for designing hemoprotein-based blood substitutes.

MATERIALS AND METHODS

Materials and Protein Samples. All reagents and chemicals were obtained from commercial sources and used as received. Sperm whale Mb was purchased as a lyophilized powder from Biozyme and used without further purification. Meso was purchased from Frontier Scientific Co. 3,8-DMD,[21,22] 7-PF,[15] and 2,8-DPF[16] were synthesized as previously described. The apoprotein of Mb was prepared at 4 °C according to the procedure of Teale,[23] and reconstituted Mbs were prepared by slow addition of a synthetic heme cofactor to the apoMb in 50 mM potassium phosphate buffer, pH 7.0, at 4 °C.[23] In order to prepare oxygenated form of Mb (oxyMb), metMb was reduced by adding $Na_2S_2O_4$ (Nakarai Chemicals Ltd.) in the presence of carbon monoxide (CO) gas (Japan Air Gases), and then the protein was freed from excess reagents by passage through a Sephadex G-10 (Sigma-Aldrich Co.) column equilibrated with an appropriate buffer solution. Finally, Fe-bound CO was replaced with O_2 by flash photolysis in the presence of O_2 gas (Japan Air Gases). The pH of each sample was measured with a Horiba F-22 pH meter equipped with a Horiba type 6069−10c electrode. The pH of the sample was adjusted using 0.1 M NaOH or HCl.

Oxygen Equilibrium Curves. An oxygen equilibrium curve (OEC) for Mb(3,8-DMD) was measured with 30 μM protein in 100 mM phosphate buffer, pH 7.4, and 100 mM Cl^- at 20 °C, using the previously described automatic oxygenation apparatus.[24,25] The P_{50} value was determined through nonlinear least-squares fitting of the OEC data.

Measurement of Autoxidation Reaction Rates. UV−vis absorption spectra were recorded for 10 μM protein samples at 35 °C using a Beckman DU 640 spectrophotometer, and 100 mM sodium acetate and potassium phosphate buffers were used to prepare sample solutions in the pH ranges of 4.1−5.8 and 5.8−7.4, respectively. Autoxidation of a protein was followed by recording UV−vis spectra over 250−750 nm using a Beckman DU 640 spectrophotometer equipped with a six-cell changer and a Peltier temperature control module. The autoxidation reactions were characterized by only two spectral species with clear isosbestic points, and the observed time evolution could be represented well by a simple first order reaction mechanism, that is, $d[\text{OxyMb}]/dt = -k_{ox}[\text{OxyMb}]$, where k_{ox} is the apparent autoxidation reaction rate constant.

Density Functional Theory Calculation. The density functional theory (DFT) calculations were carried out using the Gaussian 03 program package.[26] The restricted spin orbital approach involving the B3LYP method (spin multiplicity =1), together with electron basis sets of Pople's 6-31G(d), was employed. For simplification, the calculations were performed for the 2,3,7,8,12,13,17,18-octamethylporphinatoiron-(II) complex, and its mono- and di-CF_3- as well as divinyl-substituted derivatives as models for the heme cofactors used in this study (see Figure S1 in the Supporting Information) in order to determine the effect of the heme side-chain modifications on the H^+ affinity of Fe^{2+}-bound O_2. Geometry optimization of the porphyrin moieties of the model compounds was carried out in the gas phase[16] with a fixed CH_3 (or CF_3) and vinyl group orientation, that is, in the case of a CH_3 (or CF_3) group, one C−H (or C−F) fragment was in the porphyrin plane, and the others were pointing above and below the plane, and the vinyl one was assumed to be in the porphyrin plane with the 3(8)-vinyl C_β atom located closest to the 2(7)-CH_3 group (see Figure S1 in the Supporting Information). In addition, the oxidation, spin, and coordination states of the heme Fe atoms of the model compounds were assumed to be Fe(II), $S = 0$, and a 6-coordinated structure with imidazole and O_2 ligands, respectively. The imidazole ligand was used as the model for the proximal His93 coordinated to the heme Fe, and its orientation and the orientation of Fe^{2+}-bound O_2, with respect to the heme, were adopted from those of the imidazole moiety of the His93 side chain and O_2, respectively, determined in an X-ray crystallographic study on the native protein (PDB: 1A6M).[27] Furthermore, in the models of proto and 7-PF, only the predominant heme orientation, out of the two possible ones differing by 180° rotation about the 5-H−15-H axis, with respect to His93, in the proteins[27,28] was considered. The H^+ affinity of Fe^{2+}-bound O_2 was estimated on the basis of the gas phase acidity[29] (ΔG_{acid}) calculated as the difference in energy between the model compounds possessing protonated ($Fe^{2+}-O_2H^+$) and deprotonated ($Fe^{2+}-O_2$) states. Structural optimization was performed only for the orientation of the added proton, with respect to the Fe-bound O_2, in the protonated form (see Table S1 in the Supporting Information). In addition, vibrational analyses[30] were performed to determine the ΔG_{acid} values at 298.15 K.

dx.doi.org/10.1021/ic301848t | Inorg. Chem. 2012, 51, 11955−11960

RESULTS

O_2 Affinity of Mb(3,8-DMD). We first measured the OEC of Mb(3,8-DMD) at 20 °C and pH 7.4 (see Figure S2 in the Supporting Information), the value of 0.50 mmHg being determined for the P_{50} value of the protein (Table 1). We had previously found that the O_2 affinity of Mb decreases with decreasing ρ_{Fe} value of the protein, and demonstrated, using the P_{50} and pK_a values as measures of the O_2 affinity and the ρ_{Fe} value of the protein, respectively, that the O_2 affinity of the protein decreases with a decrease in the ρ_{Fe} value, as shown in Figure 2.[16] The linear pK_a-log($1/P_{50}$) plots in Figure 2 predicted the value of 0.54 mmHg for the P_{50} value of the protein, because the pK_a value of 9.1 ± 0.1 has been reported for the protein.[22] Consequently, the agreement between the determined and predicted P_{50} values for Mb(3,8-DMD) (Figure 2) confirmed that the O_2 affinity of the protein is regulated by the ρ_{Fe} value. Furthermore, based on the pK_a values of the proteins (Table 1), the proteins can be ranked as Mb(2,8-DPF) < Mb(7-PF) < Native Mb < Mb(3,8-DMD) ≈ Mb(Meso), in order of increasing ρ_{Fe} value (see Figure S4 in the Supporting Information).

Table 1. k_{ox}, P_{50}, log($1/P_{50}$), and pK_a Values of Mbs

Mb	k_{ox} (h^{-1})[a]	P_{50} (mmHg)[b]	log($1/P_{50}$)	pK_a[c]
Mb(Meso)	0.16 ± 0.02	0.38[d]	0.42	9.43 ± 0.03
Mb(3,8-DMD)	0.14 ± 0.01	0.50	0.30	9.1 ± 0.1[e]
Mb(7-PF)	0.051 ± 0.005	1.10[d]	−0.041	8.57 ± 0.03
Mb(2,8-DPF)	0.033 ± 0.003	2.80[d]	−0.45	7.41 ± 0.05
Native Mb	0.083 ± 0.008	0.58[d]	0.24	8.90 ± 0.05

[a]Measured at pH 7.40 and 35 °C. [b]At pH 7.40 and 20 °C (see Figure S3 in the Supporting Information). [c]At 25 °C. [d]Obtained from ref 16. [e]Obtained from ref 22.

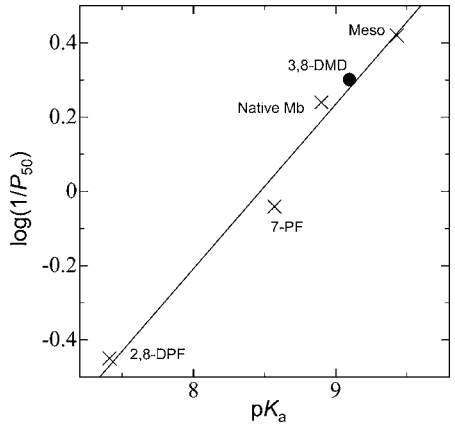

Figure 2. Plots of the pK_a values against the quantity log($1/P_{50}$) for native Mb, Mb(Meso), Mb(7-PF), and Mb(2,8-DPF), indicated by ×, and Mb(3,8-DMD), indicated by ●. The pK_a values were determined at 25 °C, and the P_{50} ones at 20 °C and pH 7.40. The data for native Mb, Mb(Meso), Mb(7-PF), and Mb(2,8-DPF) were taken from ref 16.

Autoxidation Reaction Rates of the Proteins. We next measured the autoxidation reaction rates (k_{ox}) of native Mb and the reconstituted proteins under acidic pH conditions (see Figure S5 in the Supporting Information). The pH-profiles of the k_{ox} values of the proteins under neutral to acidic pH conditions are compared with each other in Figure 3. As has been reported previously for native Mb,[31−33] the pH-profiles can be represented by straight lines with slopes of −0.5 to about −0.6, reflecting similar acid-catalysis processes for the autoxidation reactions of these proteins. The plots clearly indicated that the proteins can be ranked as Mb(2,8-DPF) < Mb(7-PF) < Native Mb < Mb(3,8-DMD) ≈ Mb(Meso), in order of increasing k_{ox} value at a given pH in the range examined. The determined ranking of the proteins is essentially identical to that of the proteins, in order of increasing ρ_{Fe} value.[16] In fact, the plots of the k_{ox} values at pH 7.40 against the pK_a values could be represented by a straight line (Figure 4A), and indicated that the k_{ox} value decreases by a factor of 1/2.2 with a decrease of 1 pK_a unit, demonstrating that the autoxidation is regulated by the ρ_{Fe} value. Considering our previous finding that the O_2 affinity of Mb decreases with a decrease in the ρ_{Fe} value,[16] it is concluded that a protein with a

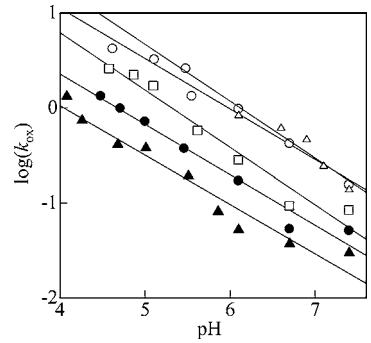

Figure 3. pH profiles of the autoxidation reaction rates (k_{ox}) of Mb(Meso) (○), Mb(3,8-DMD) (△), Mb(7-PF) (●), Mb(2,8-DPF) (▲), and native Mb (□) at 35 °C. The k_{ox} values of the proteins in 100 mM sodium acetate, pH 4.1−5.8, or potassium phosphate, pH 5.8−7.4, buffer at 35 °C were measured (see Figure S5 in the Supporting Information).

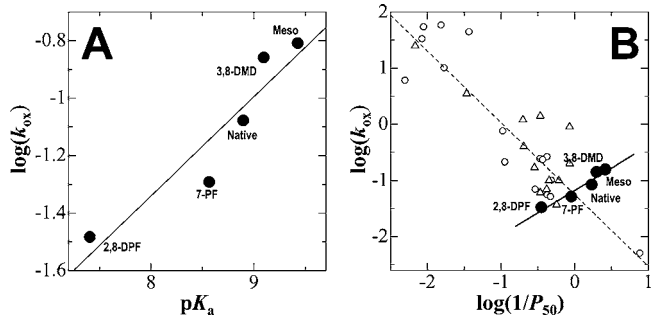

Figure 4. (A) Plots of the k_{ox} values against the pK_a ones of native Mb, Mb(Meso), Mb(3,8-DMD), Mb(7-PF), and Mb(2,8-DPF), and (B) ones of log(k_{ox}) against log($1/P_{50}$) of the proteins. The k_{ox} values of the proteins were measured at pH 7.40 and 35 °C. The P_{50} value of Mb(3,8-DMD) was measured at 20 °C and pH 7.40, and the pK_a one of the protein at 25 °C was taken from ref 22. The P_{50} and pK_a values of the other proteins were taken from ref 16. In Figure 4B, the data reported for sperm whale (open circles) and pig Mb mutants (open triangles) at pH 7.0 and 37 °C[11] were plotted in order to show the effect of amino acid replacements on the log(k_{ox}) and log($1/P_{50}$) values. The lines were drawn using least-squares fitting. Although, due to the disagreement in the experimental conditions used for the measurements, the plots of the reconstituted proteins cannot be directly compared with those of the mutant ones, it is apparent that the functional consequences of the heme side-chain modifications and amino acid replacements are different from each other.

dx.doi.org/10.1021/ic301848t | Inorg. Chem. 2012, 51, 11955−11960

Scheme 2. Reaction Mechanism[a] for Autoxidation of Mb, Subsequent to Its Oxygenation, Proposed by Shikama[34−36]

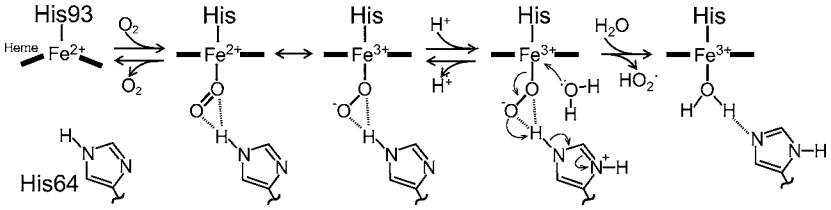

[a]Dissociation of hydroperoxyl radical $HO_2^•$ from heme Fe^{3+}, followed by instantaneous coordination of H_2O to heme Fe^{3+}, the 4th drawing, is only a speculative process, and simultaneous accommodation of both H_2O and Fe-bound O_2 hydrogen-bonded to His64 in the heme pocket of the protein would be possible.

smaller ρ_{Fe} value exhibits lower O_2 affinity and a smaller k_{ox} value, as illustrated in Figure 4B.

DISCUSSION

Correlation between the Autoxidation Reaction Rate and Electron Density of the Heme Fe Atom. The pH-profiles of the k_{ox} values of the proteins (Figure 3) indicated not only that the autoxidation becomes slower with increasing number of electron-withdrawing CF_3 groups, but also that an acid-catalysis process is operative in the autoxidation. These findings could be interpreted in terms of the molecular mechanism for autoxidation proposed by Shikama[34−36] (Scheme 2). According to Shikama's mechanism,[34−36] the acid-catalysis process occurs through protonation of Fe^{2+}-bound O_2, which leads to dissociation of hydroperoxyl radical $HO_2^•$ from the active site of the protein, followed by ionization of the $HO_2^•$ into H^+ and superoxide anion radical $O_2^{•-}$, the pK_a value being 4.8.[37] Hence, the decrease in the k_{ox} value of the protein with decreasing ρ_{Fe} value, as reflected in a lower pK_a one, can be attributed to lowering of the H^+ affinity of the Fe^{2+}-bound O_2, which in turn inhibits the production of $Fe^{3+}-O_2H$.

Upon protonation of the Fe^{2+}-bound O_2, His64 acts as an effective transporter of H^+ from the solvent to the Fe^{2+}-bound O_2, through tautomerism of its side chain imidazole hydrogen bonded to the bound ligand (Scheme 2).[34−36] Consequently, the regulation of the k_{ox} value through the ρ_{Fe} one, revealed by the present study, demonstrated that tautomerism of the His64 side chain imidazole is affected by the ρ_{Fe} value through the hydrogen bond between the Fe^{2+}-bound O_2 and His64 ("distal H-bond").

Harada et al.[38] demonstrated that interaction between His64 and heme 13-propionate side chains, via an intervening water molecule and the Arg45 side chain, contributes to inhibition of the autoxidation of the protein, possibly due to its suppressive effect on the entry of water molecules into the heme active site of the protein. Thus, the present study revealed the electronic mechanism responsible for the control of the autoxidation of the protein.

Correlation between the O_2 Affinity and Autoxidation Reaction Rate. An $Fe^{3+}-O_2^-$-like species has been expected for the $Fe^{2+}-O_2$ bond in oxyMb (Scheme 2),[39] and hence the withdrawal of electron density from the porphyrin moiety of the heme toward the electron-attracting peripheral side chains is thought to hinder the formation of this $Fe^{3+}-O_2^-$-like species through obstruction of Fe−O bond polarization. Since O_2 dissociation from the heme Fe atom is thought to occur only at the $Fe^{2+}-O_2$ bond, stabilization of the $Fe^{2+}-O_2$ bond over the $Fe^{3+}-O_2^-$-like one with increasing number of electron-withdrawing CF_3 groups should result in an increase in the O_2 dissociation rate,[16] which would lower the O_2 affinity. Furthermore, since the H^+ affinity of the Fe^{2+}-bound O_2 is thought to be lower than that of the $Fe^{3+}-O_2^-$-like form, the stabilization of the former over the latter with CF_3 substitution should inhibit the acid-catalysis process for the autoxidation of the protein, resulting in a decreased k_{ox} value.

We have estimated the H^+ affinity of Fe^{2+}-bound O_2 through DFT calculations using the Gaussian 03 program package.[26] Gas phase acidity (ΔG_{acid}) calculated as the difference in energy between model compounds possessing protonated ($Fe^{2+}-O_2H^+$) and deprotonated ($Fe^{2+}-O_2$) states was used as a measure for the H^+ affinity of Fe^{2+}-bound O_2 (Table 2). The results indicated that the ΔG_{acid} value decreases with increasing number of CF_3 groups, suggesting that the H^+ affinity of Fe^{2+}-bound O_2 decreases with decreasing ρ_{Fe} value (see Figure S3 in the Supporting Information). Consequently, the results of the DFT calculations supported that the decrease in the k_{ox} value upon CF_3 substitution is due to the inhibition of the acid-catalysis process for the autoxidation of the protein as a result of decreasing H^+ affinity of the Fe^{2+}-bound O_2.

Table 2. Gas Phase Acidity (ΔG_{acid}) of the Model Compounds[a]

Model	R_2	R_3	R_7	R_8	ΔG_{acid} (kJ mol^{-1})
Model for Meso and 3,8-DMD	CH_3	CH_3	CH_3	CH_3	−1019.95
Model for 7-PF	CH_3	CF_3	CH_3	CH_3	−996.29
Model for 2,8-DPF	CF_3	CH_3	CH_3	CF_3	−971.88
Model for Proto	CH_3	$CH=CH_2$	CH_3	$CH=CH_2$	−1002.81

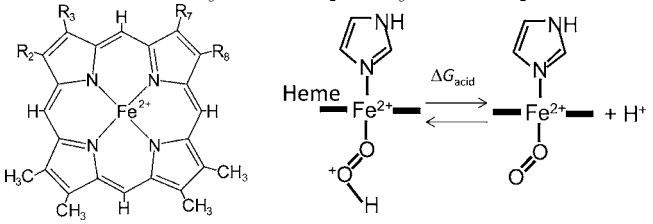

[a]Structures of the model compounds are illustrated below and the ΔG_{acid} value was calculated as the difference in energy between the $Fe^{2+}-O_2H^+$ and $Fe^{2+}-O_2$ states (see also text and Figure S1 and Table S1 in the Supporting Information for details).

As described above, CF_3 substitution influences the resonance process between the $Fe^{2+}-O_2$ bond and $Fe^{3+}-O_2^-$-like species in oxyMb (Scheme 2). A shift of the resonance toward the $Fe^{2+}-O_2$ form results in lowering of the O_2 affinity due to an increase in the O_2 dissociation rate.[16] On the other hand, a shift of the resonance toward the $Fe^{3+}-O_2^-$-like species results in acceleration of the autoxidation through increasing

dx.doi.org/10.1021/ic301848t | Inorg. Chem. 2012, 51, 11955−11960

H^+ affinity of the bound ligand. Consequently, the resonance process between the $Fe^{2+}-O_2$ bond and $Fe^{3+}-O_2^-$-like species appears to act as an electronic switch that determines the fate of oxyMb.

On the basis of detailed theoretical investigations, Chen et al.[40] revealed the importance of the distal H-bond in determining nature of the $Fe^{2+}-O_2$ bonding in the protein. The strength of the distal H-bond is expected to be affected by a shift in the resonance process between the $Fe^{2+}-O_2$ bond and $Fe^{3+}-O_2^-$-like species (Scheme 2). However, it is not clear at present to what extent the strength of the distal H-bond is affected by the shifts the resonance process due to the heme side-chain modifications examined in the study.

We have shown that Mb possessing a smaller (larger) ρ_{Fe} value exhibits lower (higher) O_2 affinity and a smaller (larger) k_{ox} value. In contrast, it was demonstrated, in the studies on artificial mutants, that a mutant possessing lower (higher) O_2 affinity exhibits a larger (smaller) k_{ox} value (Figure 4B).[4,11−14] Thus, the functional consequences of perturbation of the heme electronic structure, through chemical modification of the peripheral side chain(s), and that of the protein structure, through amino acid replacement(s), are completely different from each other. This can be explained in terms of the effects of the perturbations on the properties of oxyMb. In the case of the electronic perturbation through changes in the ρ_{Fe} value, the O_2 affinity and k_{ox} value are regulated through a shift in the resonance process between the $Fe^{2+}-O_2$ bond and $Fe^{3+}-O_2^-$-like species in oxyMb, as described above. On the other hand, the structural perturbation of the protein through amino acid replacement(s) influences the stability of oxyMb itself, and the resonance process between the $Fe^{2+}-O_2$ bond and $Fe^{3+}-O_2^-$-like species is unlikely to be affected by any perturbation. Consequently, a decrease (an increase) in the stability of oxyMb caused by amino acid replacement(s) should result in increases (decreases) in both the O_2 dissociation rate, leading to lower O_2 affinity, and the k_{ox} value. Therefore, the combined use of the two perturbations allows us to independently control the O_2 affinity and autoxidation rate of the protein. This finding provided a new way for designing hemoprotein-based blood substitutes.

■ ASSOCIATED CONTENT

Ⓢ Supporting Information

Model compounds subjected to DFT calculations and the obtained results, OEC for Mb(3,8-DMD), and experimental details of the determination of the autoxidation reaction rate constants of the proteins. This material is available free of charge via the Internet at http://pubs.acs.org.

■ AUTHOR INFORMATION

Corresponding Author

*Phone/Fax: +81 29 853 6521. E-mail: yamamoto@chem.tsukuba.ac.jp.

Notes

The authors declare no competing financial interest.

■ ACKNOWLEDGMENTS

This work was supported by a Grants-in-Aid for Scientific Research on Innovative Areas (Nos. 23108703, "π-Space") from the Ministry of Education, Culture, Sports, Science and Technology, Japan, the Yazaki Memorial Foundation for Science and Technology, and the NOVARTIS Foundation (Japan) for the Promotion of Science.

■ REFERENCES

(1) Chu, K.; Vojtchovsky, J.; McMahon, B. H.; Sweet, R. M.; Berendzen, J.; Schlichting, I. *Nature* **2000**, *403*, 921−923.
(2) Schotte, F.; Lim, M.; Jackson, T. A.; Smirnov, A. V.; Soman, J.; Olson, J. S.; Phillips, G. N., Jr.; Wulff, M.; Anfinrud, P. A. *Science* **2003**, *300*, 1944−1947.
(3) Antonini, E.; Brunori, M. In *Hemoglobins and Myoglobins and their Reactions with Ligands*; North Holland Publishing: Amsterdam, 1971.
(4) Springer, B. A.; Sligar, S. G.; Olson, J. S.; Phillips, G. N., Jr. *Chem. Rev.* **1994**, *94*, 699−714.
(5) Olson, J. S.; Phillips, G. N., Jr. *J. Biol. Inorg. Chem.* **1997**, *2*, 544−552.
(6) Capece, L.; Marti, M. A.; Crespo, A.; Doctorvich, F.; Estrin, D. A. *J. Am. Chem. Soc.* **2006**, *128*, 12455−12461.
(7) Tomita, A.; Sato, T.; Ichiyanagi, K.; Nozawa, S.; Ichikawa, H.; Chollet, M.; Kawai, F.; Park, S.-Y.; Tsuduki, T.; Yamato, T.; Koshihara, S.-Y.; Adachi, S. *Proc. Natl. Acad. Sci. U.S.A.* **2009**, *106*, 2612−2616.
(8) Miele, A. E.; Santanché, S.; Travaglini-Allocatelli, C.; Vallone, B.; Brunori, M.; Bellelli, A. *J. Mol. Biol.* **1999**, *290*, 515−524.
(9) George, P.; Stratmann, C. J. *Biochem. J.* **1954**, *57*, 568−573.
(10) Livingston, D. J.; McLachlan, S. J.; La Mar, G. N.; Brown, W. D. *J. Biol. Chem.* **1985**, *260*, 15699−15707.
(11) Brantly, R. E.; Smerdon, S. J.; Wilkinson, A. J.; Singleton, E. W.; Olson, J. S. *J. Biol. Chem.* **1993**, *268*, 6995−7010.
(12) Carver, T. E.; Brantley, R. E., Jr.; Singleton, E. W.; Arduini, R. M.; Quillin, M. L.; Phillips, G. N., Jr.; Olson, J. S. *J. Biol. Chem.* **1992**, *267*, 14443−14450.
(13) Zhao, X.; Vyas, K.; Nguyen, B. D.; Rajarathnam, K.; La Mar, G. N.; Li, T.; Phillips, G. N., Jr.; Eich, R. F.; Olson, J. S.; Ling, J.; Bocian, D. F. *J. Biol. Chem.* **1995**, *270*, 20763−20774.
(14) Springer, B. A.; Egeberg, K. D.; Sligar, S. G.; Rohlfs, R. J.; Mathews, A. J.; Olson, J. S. *J. Biol. Chem.* **1989**, *264*, 3057−3060.
(15) Toi, H.; Homma, M.; Suzuki, A.; Ogoshi, H. *J. Chem. Soc., Chem. Commun.* **1985**, 1791−1792.
(16) Shibata, T.; Nagao, S.; Fukaya, M.; Tai, H.; Nagatomo, S.; Morihashi, K.; Matsuo, T.; Hirota, S.; Suzuki, A.; Imai, K.; Yamamoto, Y. *J. Am. Chem. Soc.* **2010**, *132*, 6091−6098.
(17) Pande., U.; La Mar, G. N.; Lecomte, J. T. L.; Ascoli, F.; Brunori, M.; Smith, K. M.; Pandey, R. K.; Parish, D. W.; Thanabal, V. *Biochemistry* **1986**, *25*, 5638−5646.
(18) Yamamoto, Y.; Osawa, A.; Inoue, Y.; Chûjô, R.; Suzuki, T. *Eur. J. Biochem.* **1990**, *192*, 225−229.
(19) Yamamoto, Y.; Chûjô, R.; Inoue, Y.; Suzuki, T. *FEBS Lett.* **1992**, *310*, 71−74.
(20) Nagao, S.; Hirai, Y.; Suzuki, A.; Yamamoto, Y. *J. Am. Chem. Soc.* **2005**, *127*, 4146−4147.
(21) Chang, C. K; Ward, B.; Ebina, S. *Arch. Biochem. Biophys.* **1984**, *231*, 366−371.
(22) Neya, S.; Suzuki, M.; Hoshino, T.; Ode, H.; Imai, K.; Komatsu, T.; Ikezaki, A.; Nakamura, M.; Furutani, Y.; Kandori, H. *Biochemistry* **2010**, *49*, 5642−5650.
(23) Teale, F. W. J. *Biochim. Biophys. Acta* **1959**, *35*, 543.
(24) Imai, K. *Methods Enzymol.* **1981**, *76*, 438−449.
(25) Imai, K. *Methods Enzymol.* **1981**, *76*, 470−486.
(26) Frisch, M. J.; Trucks, G. W.; Schlegel, H. B.; Scuseria, G. E.; Robb, M. A.; Cheeseman, J. R.; Montgomery, J. A., Jr.; Vreven, T.; Kudin, K. N.; Burant, J. C.; Millam, J. M.; Iyengar, S. S.; Tomasi, J.; Barone, V.; Mennucci, B.; Cossi, M.; Scalmani, G.; Rega, N.; Petersson, G. A.; Nakatsuji, H.; Hada, M.; Ehara, M.; Toyota, K.; Fukuda, R.; Hasegawa, J.; Ishida, M.; Nakajima, T.; Honda, Y.; Kitao, O.; Nakai, H.; Klene, M.; Li, X.; Knox, J. E.; Hratchian, H. P.; Cross, J. B.; Bakken, V.; Adamo, C.; Jaramillo, J.; Gomperts, R.; Stratmann, R. E.; Yazyev, O.; Austin, A. J.; Cammi, R.; Pomelli, C.; Ochterski, J. W.; Ayala, P. Y.; Morokuma, K.; Voth, G. A.; Salvador, P.; Dannenberg, J. J.; Zakrzewski, V. G.; Dapprich, S.; Daniels, A. D.; Strain, M. C.; Farkas, O.; Malick, D. K.; Rabuck, A. D.; Raghavachari, K.; Foresman,

J. B.; Ortiz, J. V.; Cui, Q.; Baboul, A. G.; Clifford, S.; Cioslowski, J.; Stefanov, B. B.; Liu, G.; Liashenko, A.; Piskorz, P.; Komaromi, I.; Martin, R. L.; Fox, D. J.; Keith, T.; Al-Laham, M. A.; Peng, C. Y.; Nanayakkara, A.; Challacombe, M.; Gill, P. M. W.; Johnson, B.; Chen, W.; Wong, M. W.; Gonzalez, C.; Pople, J. A. *Gaussian 03*, Revision E.01; Gaussian, Inc.: Wallingford, CT, 2004.
(27) Vojtechovský, J.; Chu, K.; Berendzen, J.; Sweet, R. M.; Schlichting, I. *Biophys. J.* **1999**, *77*, 2153−2174.
(28) Yamamoto, Y.; Nagao, S.; Hirai, Y.; Inose, T.; Terui, N.; Mita, H.; Suzuki, A. *J. Biol. Inorg. Chem.* **2004**, *9*, 152−160.
(29) Koppel, I. A.; Burk, P.; Koppel, I.; Leito, Ivo; Sonoda, T.; Mishima, M. *J. Am. Chem. Soc.* **2000**, *122*, 5114−5124.
(30) McQuarrie, D. A. In *Statistical Thermodynamics*; Wiley and Sons: New York, 1973.
(31) Suzuki, T.; Shikama, K. *Arch. Biochem. Biophys.* **1983**, *224*, 695−699.
(32) Shikama, K.; Matsuoka, A. *Biol. Rev.* **1994**, *69*, 233−251.
(33) Shikama, K.; Sugawara, Y. *Eur. J. Biochem.* **1978**, *91*, 407−413.
(34) Sugawara, Y; Shikama, K. *Eur. J. Biochem.* **1980**, *110*, 241−246.
(35) Shikama, K. *Coord. Chem. Rev.* **1988**, *83*, 73−91.
(36) Shikama, K. *Prog. Biophys. Mol. Biol.* **2006**, *91*, 83−162.
(37) Bielski, B. H. J; Allen, A. O. *J. Phys. Chem.* **1977**, *81*, 1048−1050.
(38) Harada, K; Makino, M.; Sugimoto, H.; Matsuo, T.; Shiro, Y.; Hisaeda, Y.; Hayashi, T. *Biochemistry* **2007**, *46*, 9406−9416.
(39) Maxwell, J. C.; Volpe, J. A.; Barlow, C. H.; Caughey, W. S. *Biochem. Biophys. Res. Commun.* **1974**, *58*, 166−171.
(40) Chen, H.; Ikeda-Saito, M.; Shaik, S. *J. Am. Chem. Soc.* **2008**, *130*, 14778−14790.